Journal of Nuclear Materials 390–391 (2009) 806–809

Contents lists available at ScienceDirect

Journal of Nuclear Materials

journal homepage: www.elsevier.com/locate/jnucmat

Analysis of radiative disruptions in RF-heated Tore Supra plasmas using infrared imaging

A. Ekedahl *, J. Bucalossi, Y. Corre, E. Delchambre, G. Dunand, O. Meyer, R. Mitteau, P. Monier-Garbet, B. Pégourié, F.G. Rimini, F. Saint-Laurent, J.L. Schwob, E. Tsitrone

CEA, IRFM, F-13108 Saint-Paul-lez-Durance, France

ARTICLE INFO

PACS:
52.55.Fa

ABSTRACT

The precursors and following sequential events leading to radiative disruptions in Tore Supra have been analysed using infrared imaging, together with visible and ultraviolet spectroscopy of impurity species. A common feature observed prior to the disruptions is the appearance of a small ($\sim$cm^2) hot spot on the main plasma facing component, the Toroidal Pumped Limiter (TPL), clearly localised in a zone of thick carbon re-deposition (>100 μm). A MARFE (Multifaceted Asymmetric Radiation From the Edge) is often triggered, followed by disruption. Such hot spots have been observed in $\sim$24% of the analysed disruptions, which is consistent with the fact that only 4/18 (22%) of the total area of the TPL is monitored with infrared cameras. These results suggest that over-heating of thick carbon re-deposition layers may play a role in the operational limits (MARFE, disruption) encountered.

1. Introduction

The Tore Supra tokamak has a unique long pulse capability in an actively cooled machine, with injected power provided exclusively by radiofrequency (RF) waves. The last two years experimental campaigns have been particularly intense in terms of injected power, energy and accumulated plasma time (10 h plasma time in both 2006 and 2007, with 65GJ injected RF energy in 2006 and 40GJ in 2007). Large experience has been gained in the understanding of localised heat loads due to RF sheath effects and interaction by fast particles [1,2]. In addition, a unique experimental campaign dedicated to fuel retention studies [3] allows to assess the evolution of plasma parameters and wall conditioning, as well as the reliability of the technical installations, during repetitive and identical, long duration discharges.

However, an increasing operational difficulty has emerged during the recent campaign, limiting the high power and long pulse performance. This limitation is related to the formation of a MARFE, usually leading to a disruption. Generally, the MARFE onset depends on impurity radiation and is therefore dependent on wall conditions and limiter materials [4,5]. Processes involving recycling of neutral hydrogen have also been reported to play a role [6]. The analysis presented in this paper shows that the MARFE and disruption in several cases is preceded by a localised hot spot in a region of thick carbon re-deposition on the main plasma facing component, the toroidal pumped limiter (TPL). These deposits accumulate in the shadowed zones on the TPL and have grown over several experimental campaigns since the installation of the TPL in 2000. A deposit thickness of $\sim$100–200 μm has been estimated [7]. The experimental observations indicate that over-heating and possibly flaking of these deposits could play a role in the operational limits encountered.

2. Experimental conditions

The two main experimental scenarios used during the campaigns, and analysed for this work, are the following: The first scenario, aiming at high power long duration discharges, consisted of a combination of lower hybrid current drive (LHCD) and ion cyclotron resonance heating (ICRH), at high plasma current and density (I_P = 0.8–1.0 MA and $n_e/n_G \sim 0.8$). This has resulted in 9.5 MW coupled for $\sim$30 s in repetitive discharges [1,8]. The second scenario, aiming at loading the vessel walls with deuterium in a campaign dedicated to fuel retention studies [3], used pure LHCD discharges at 2 MW up to 120 s at I_P = 0.6 MA and $n_e/n_G \sim 0.5$. A particularity of this scenario was that no conditioning was carried out during the ten days experiment. This corresponded to 5 h of plasma, which is roughly equal to one normal year of plasma operation in Tore Supra.

In the steady-state phase of the discharges, the radiation pattern (mainly due to carbon) is poloidally asymmetric, with its maximum localised near the surface of the TPL, at the bottom of the torus. In both scenarios a sudden, strong increase in radiation and the formation of a MARFE was observed, as indicated by a rapid shift of the radiation maximum from the TPL towards the high

* Corresponding author.
E-mail address: annika.ekedahl@cea.fr (A. Ekedahl).

0022-3115/$ - see front matter © 2009 Elsevier B.V. All rights reserved.
doi:10.1016/j.jnucmat.2009.01.213

field side [8]. These radiation events have been analysed using infrared (IR) imaging as the main tool. IR cameras view almost 4 out of the 18 toroidal TPL sectors. Each of the five RF antennas (two LHCD and three ICRH) are also monitored by IR cameras, which allow to distinguish specific phenomena related e.g. to arcs on front of the waveguides. To complement the IR analysis of the TPL, visible spectroscopy of one TPL sector (named Q6B) allows to measure the Hα-emission (6563 Å) and CII-emission (6578 Å) along four lines-of-sight [9]. In addition, ultraviolet (UV) spectroscopy measurements (CIV, OIV and FeXV) are made along an equatorial line of sight [10].

3. Analysis of radiative disruptions

More than 140 disruptions have been analysed using IR imaging. A common feature observed prior to the disruptions is the appearance of a small ($\sim$cm^2) hot spot, clearly localised in a zone of thick carbon re-deposition on the TPL. Fig. 1 shows the time evolution of the main plasma parameters during a discharge with 7 MW of additional heating power. All parameters remain constant from 10 s to 14.6 s, with a radiated power fraction of $P_{Rad}/P_{Tot} \sim 22\%$. At 14.6 s, a hot spot appears in the carbon re-deposition region on the high field side (HFS) of the TPL, as revealed by the high resolution IR camera (Fig. 2(a)). The images in Fig. 2 represent the temperature difference with respect to 14.5 s, thus illustrating the localised structure of the hot spot. During the following $\sim$100 ms, the hot spot grows and shifts towards the HFS edge of the TPL (Fig. 2(b)). This is accompanied by a small increase in electron density and radiated power, as seen in Fig. 1. At 14.7 s, a MARFE is triggered, as seen on the radiation maximum which shifts from the LPT towards the high field side. A strong increase in impurity emission (FeXV, CIV and OIV) can then be observed, since the impurity emission enters into the line of sight of the spectrometer (equatorial plane). The IR image in Fig. 2(c), taken at the MARFE onset, shows a largely extended hot spot as well as ejection of flakes from the over-heated zone. During the MARFE, the coupling characteristics for the RF antennas change and the heating power is reduced by the antenna protection systems. A disruption often occurs as the radiated power exceeds the input power.

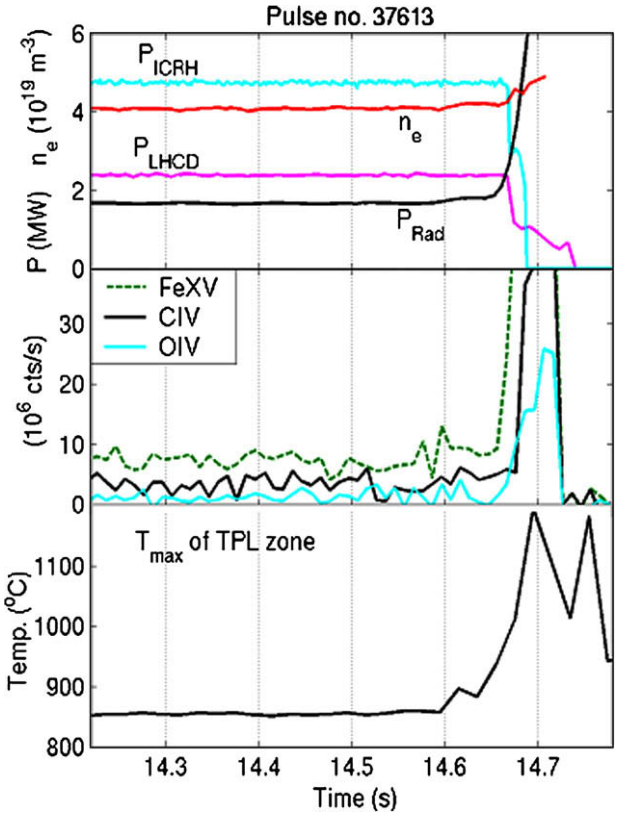

Fig. 1. Time evolution of plasma parameters during discharge #37613, exhibiting a hot spot on the TPL and terminating in disruption. The temperature trace corresponds to the maximum temperature of the observed area on the TPL.

For each disruption exhibiting a hot spot, the toroidal and poloidal location of the TPL tile where the hot spot was first detected was identified. The hot spot locations were then all brought into the same figure, showing one TPL sector, in order to get an overview for the two experimental scenarios. The result is shown in Fig. 3. In the first scenario, characterised by high power RF heating at high plasmas current, the distribution of the hot spots is quite equal between the outer and inner zones of thick carbon re-deposition (Fig. 3(a)). A hot spot was found in 20 out of the 84 disruptions analysed (i.e. $\sim$24%). This is consistent with the fact that almost 4 out of the 18 TPL sectors (i.e. $\sim$22%) are viewed by IR cameras.

In the scenario with pure LHCD at lower plasma current, the hot spots clearly occurred on the inner carbon deposit zone, close to the HFS of the TPL (Fig. 3(b)). A total of 59 disruptions were analysed. Localised hot spots were observed in 12 disruptions (i.e. $\sim$20%). From the 59 disruptions one could remove ten, which were rather due to the formation of an arc in front of the grill mouth on the LHCD launchers following the detachment of a carbon flake from the launcher side protections. The percentage of disruptions with a hot spot then becomes $\sim$24%. In this second scenario, it could be well identified that the hot spot originated at the border between the heat flux zone and the private zone. In some cases the hot spot originated from a region close to the plasma contact point. On the TPL surface, this particular zone is parallel to the magnetic field. A general theory is lacking for this case and different ad-hoc assumptions are introduced in the models to reproduce the experimental measurements of the heat flux and re-deposition patterns [11,12].

The difference in hot spot location in the two different scenarios could possibly be due to the different heating methods, i.e. ICRH + LHCD versus LHCD only. Alternatively, it could be due to the fact that the wetted area of the TPL is larger at high plasma current, thus extending closer to the re-deposition region near the LFS of the TPL.

4. Localised impurity radiation during hot spots

A visible spectroscopy system with four lines-of-sight views one TPL sector, named Q6B. Fig. 4(a) shows the IR image of the TPL sector Q6B for the discharge #38108 at 21.2 s, which is before a hot spot has occurred. The footprint (approximate) of the visible spectroscopy lines-of-sight are indicated in the IR image. Chords no. 1 and 4 are close to the HFS of the TPL. Chords no. 2 and 4 cover the outer and the inner carbon re-deposition zones, respectively, while chords no. 1 and 3 cover the inner and outer heat flux zones. Fig. 4(b) shows the temperature increase on the TPL sector Q6B in the discharge #38108 at 21.65 s, when a hot spot has developed on the inner carbon re-deposition zone. An increase in the CII-emission along chord no. 4, i.e. the chord viewing the hot spot, is observed (Fig. 5). The first peak in the CII-signal corresponds to the hot spot or the MARFE and the second peak, that affects all four chords, corresponds to the disruption following the hot spot. All the discharges exhibiting a hot spot in Q6B show a strong increase in CII-emission, either along chord no. 2 or no. 4, depending on the location of the hot spot (outer or inner carbon re-deposition zone). However, since the local temperature of the surface at the hot spot can increase to $\sim$1800 °C, Planck radiation affects the visible

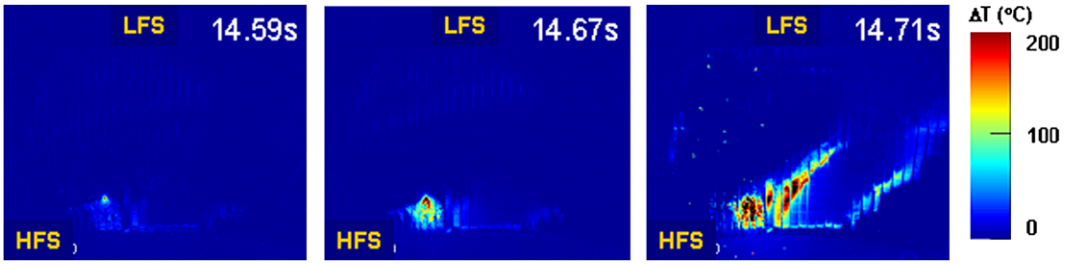

Fig. 2. Temperature difference of the hot spot, with respect to the temperature at 14.5 s, at three different times before the disruption in #37613.

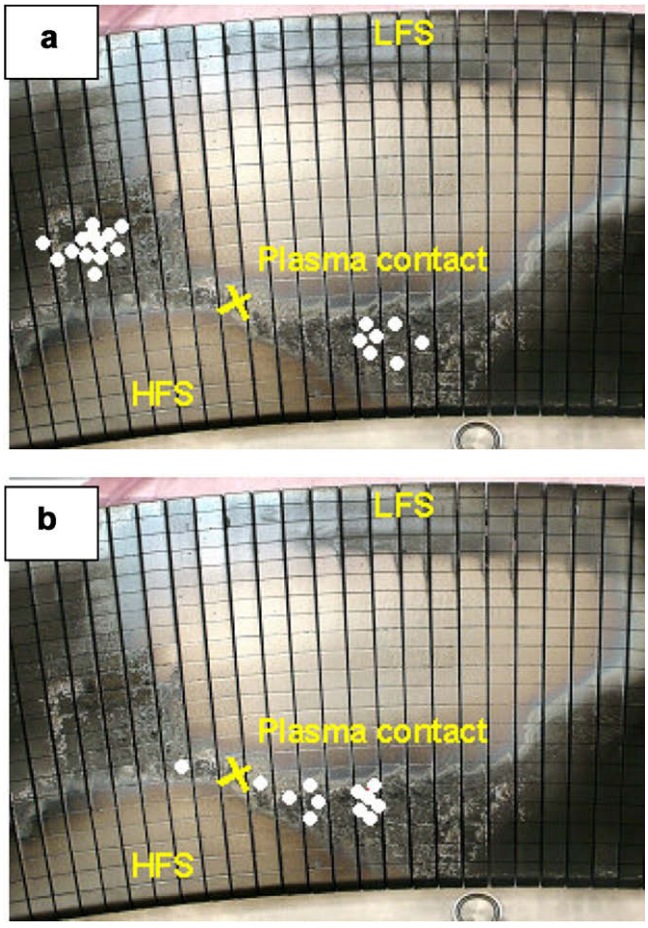

Fig. 3. Distribution of hot spots preceding the disruptions. (a) High power RF heating at I_P = 0.8–1.0 MA. (b) Pure LHCD discharges at I_P = 0.6 MA.

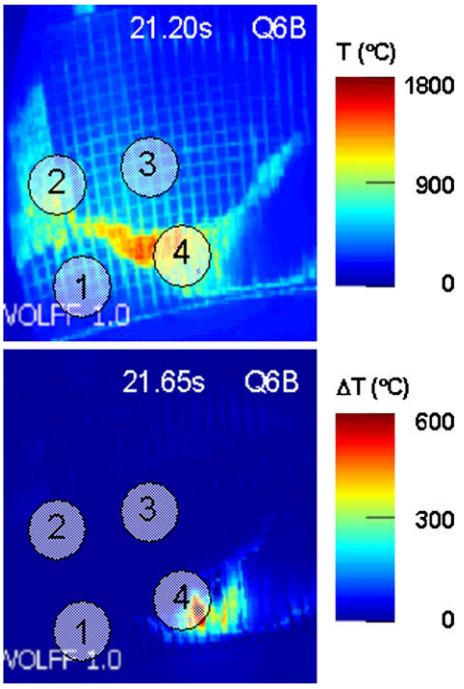

Fig. 4. (a) IR image of the TPL sector Q6B in pulse #38108, before the hot spot occurs. The four lines-of-sight of the visible spectroscopy system are also indicated. (b) IR image of the same TPL sector in pulse #38108, when the hot spot has appeared. The image shows the temperature difference with respect to the time frame in (a).

spectroscopy measurements [13]. The background level of the spectrum has therefore been subtracted in order not to overestimate the CII- and Hα-emission.

The reason for the different temperature increase of the hot spots (~300 °C in Fig. 1 and ~800 °C in Fig. 5) could possibly be due to different structure of the deposits, such as thickness or thermal contact with the TPL surface.

5. Evolution during the deuterium wall loading campaign

During the deuterium wall loading campaign, identical discharges were carried out during ten days without any conditioning in between. A carbonisation and boronisation were carried out before the start of the experiment. During the first ~3000 s of plasma, the concentration of FeXV and OIV increased continuously to return to the pre-boronisation level, while the CIV concentration and the radiated power remained constant [3,10]. This indicates that the radiated power was dominated by carbon. As described in [3], the main operational limit encountered during this campaign was the increasing frequency of radiation events, defined as $\Delta P_{Rad} > 20\%$, as well as an increasing frequency of disruptions.

Several cases of localised hot spots on the TPL were observed before the disruptions, as described in Section 3 and Fig. 3(b). When the hot spot appeared on the TPL sector Q6B, a strong burst in the CII-emission along chord no. 4 (inner re-deposition zone) was observed, in a similar way as the discharge presented in Figs. 4 and 5. Furthermore, in addition to the burst in CII-emission during the MARFE, an evolution of the Hα-emission during the steady phase of the discharge was observed along the campaign. This is shown in Fig. 6. The first disruption exhibiting a hot spot on the TPL was #39853 and the increase of the Hα-signal on chord no. 4 (inner re-deposition zone) seems to begin after the first disruption with hot spot. In contrast, the Hα-signal along chord no. 2, which views the outer re-deposition zone, does not evolve during the campaign. This is consistent with Fig. 3(b) that shows that hot spots were not occurring in this zone. As can be seen in Fig. 6,

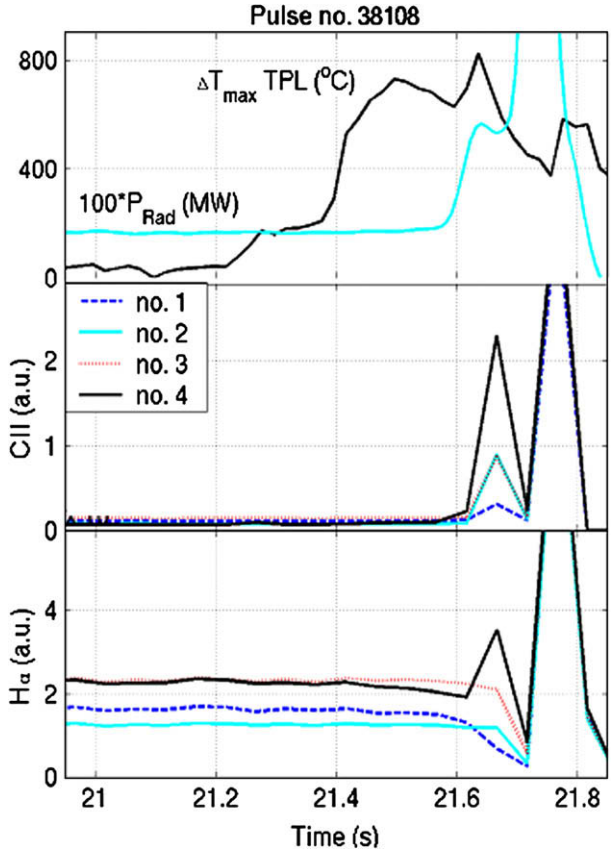

Fig. 5. Time evolution of the CII- and Hα-emission on the TPL sector Q6B in pulse #38108.

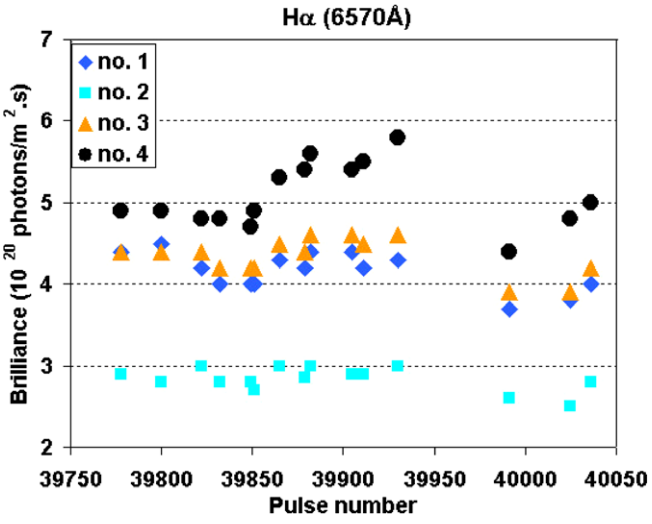

Fig. 6. Evolution of the Hα-emission in Q6B during the deuterium wall loading campaign, measured during the stationary phase of the discharges. An increase is seen on chord no. 4, which corresponds to the location of the hot spots. The decrease in Hα-emission after #39950 is due to a reduction in LHCD power.

the Hα-emission decreases again after #39950. This is due to a reduction of the LHCD power, which was necessary in order to be able to run through the discharges without disruption. Consequently, the frequency of radiation events as well as the disruption frequency decreased after having reduced the LHCD power from 2 MW to 1.5–1.8 MW [3].

6. Discussion

The experimental results presented here suggest that overheating of the re-deposited carbon layers may play a role in the operational limitations observed. The appearance of localised hot spots in the re-deposition regions resembles the observation of the so-called 'super-brilliance' events, made several years ago in Tore Supra [14]. Characteristic for those were that they occurred at locations with defective limiter tiles. To draw a parallel with the present Tore Supra configuration, the interface between the heat flux zone and the re-deposition zone on the TPL could represent such a defect. It is indeed in this region that several of the hot spots are first detected. Thermal loads can be expected due to radiation and charge exchange losses, as well as convected power close to the interface with the heat flux zone. A possible explanation for the triggering of the MARFE is that flakes detach from the overheated zone, as a result of inner thermal stresses under these thermal loads [8]. This hypothesis is also supported by an extensive analysis of the CCD images from the deuterium wall loading campaign, which indicate that most of the flaking events originate from the TPL [15].

7. Summary and outlook

An extensive analysis of IR images for Tore Supra discharges, terminating in MARFE and disruption, has been carried out. The analysis reveals that the disruption in several cases is preceded by a hot spot, clearly localised in a zone of thick carbon re-deposition on the toroidal pumped limiter (TPL). The carbon deposits on the TPL and on all other main plasma facing components were completely removed during the winter shutdown 2007–2008. The first experiments carried out in 2008, after the removal of the deposits, indicate an improved power handling and a rapid increase of the injected power capability up to 12 MW, without a single disruption. These preliminary results suggest that flaking of the carbon re-deposition layers did play a role in the operational limits encountered earlier. Further experiments will be carried out to confirm these results.

Acknowledgments

The authors gratefully acknowledge the support of the Tore Supra Team, in particular of the Radiofrequency Heating Group and the Infrared Diagnostics Group. This work, supported by the European Communities under the contract of Association between EURATOM and CEA, was carried out within the framework of the European Fusion Development Agreement. The view and opinions expressed herein do not necessarily reflect those of the European Commission.

References

[1] A. Ekedahl et al., Radiofrequency Power in Plasmas (Proceedings of Seventeenth Topical Conference, Clearwater, Florida, 2007), AIP Conference Proceedings. 933 (2007) 237.
[2] L. Colas et al., Plasma Phys. Control. Fus., 49 (2007) B35.
[3] B. Pégourié et al., J. Nucl. Mater. 390–391 (2009) 550.
[4] M. Greenwald, Plasma Phys. Control. Fus., 44 (2002) R27.
[5] J. Rapp et al., J. Nucl. Mater. 290–293 (2001) 1148.
[6] M.Z. Tokar et al., J. Nucl. Mater. 266–269 (1999) 958.
[7] R. Mitteau et al., J. Nucl. Mater. 363–365 (2007) 206.
[8] J. Bucalossi et al., in; Proceedings of Thirty-fourth EPS Conference on Plasma Physics, ECA vol. 31F, Warsaw, 2007, p. 5.113).
[9] E. Delchambre et al., J. Nucl. Mater. 390–391 (2009) 65.
[10] O. Meyer et al., J. Nucl. Mater. 390–391 (2009) 1013.
[11] R. Mitteau et al., J. Nucl. Mater. 337–339 (2005) 795.
[12] S. Carpentier et al., J. Nucl. Mater. (2008), submitted for publication.
[13] M. Stamp et al., J. Nucl. Mater. 337–339 (2005) 1038.
[14] D. Guilhem et al., J. Nucl. Mater. 241–243 (1997) 542.
[15] S. Hong et al., J. Nucl. Mater. (2008), submitted for publication.